Wideband group velocity independent coupling into slow light silicon photonic crystal waveguide

Che-Yun Lin,[1,a)] Xiaolong Wang,[2,b)] Swapnajit Chakravarty,[2] Beom Suk Lee,[1] Wei-Cheng Lai,[1] and Ray T. Chen[1,c)]
[1]*Department of Electrical and Computer Engineering, The University of Texas at Austin, Austin, Texas 78712, USA*
[2]*Omega Optics Inc., Austin, Texas 78759, USA*

We experimentally demonstrate efficient optical coupling into a slow light photonic crystal waveguide (PCW) that is independent of the group velocity of the guided mode. With a group index taper to match the group velocity between a strip waveguide and a PCW, the optical coupling efficiency is nearly constant throughout the spectrum of the defect-mode, including the slow light region near the band edge. Compared to strip-PCW butt-coupling without a group index taper, our measurement results show a 20 dB enhancement in coupling efficiency with 5 dB less Fabry–Perot fluctuations. The measurements show excellent agreement with two-dimensional finite-difference time domain simulations. © *2010 American Institute of Physics*. [doi:10.1063/1.3513814]

Slow light in photonic crystal waveguides (PCWs) can significantly enhance light-matter interaction,[1] which is a promising approach toward realizing advanced photonic devices such as tunable delay lines,[2] ultracompact optical switches,[3] and highly-efficient modulators.[4–8] To fully utilize the benefits of the slow light effect, it is crucial to efficiently couple in and out of PCW from external optical devices. However, coupling between a strip waveguide and a slow light PCW is challenging. Due to the apparent mismatch in group velocity between the fast light in the strip waveguide and the slow light in the guided mode of PCW, coupling becomes increasingly inefficient when approaching the slow light region, which limits the usefulness of slow light in practical applications. Numerous efforts have been made to address this issue. It has been reported that coupling to the defect mode away from the band edge can improve significantly with an optimized termination of the photonic crystal (PC)-strip waveguide interface;[9] however, this approach lowers coupling efficiency near the band edge, where the guided mode starts to show reduced group velocity.[10] Designing a PCW as a quarter wave transformer[11] can couple light into the slow light mode but the narrow band nature of the transformer will limit its usage in practical applications. Hetero-group velocity PCWs have demonstrated coupling into slow light mode with improved bandwidth;[12] however, its footprint is several hundred micrometers, which compromises the compactness of PC devices. Alternatively, PC injectors can provide efficient coupling for group indices up to 400 with very compact coupling structures[13] but no experimental evidence has been reported to support the feasibility of this approach. By contrast, an adiabatic transition in PCW, commonly used for improving conventional waveguide transmission, has shown good potential for efficient coupling into PCW[14,15] with a very compact coupling structure.[16] Recently, two-dimensional (2D) finite-difference time domain (FDTD) analysis shows that efficient coupling can be achieved over

the entire guided mode spectrum even in slow light modes near the band edge.[17] These characteristics make adiabatic transition in PCW a promising approach, which should be further studied experimentally for developing compact and efficient coupling structures.

In this letter, we present the design and experimental demonstration of efficient and wavelength-independent coupling into slow light PCW using two parabolic PC tapers with gradually changed air hole diameters. Based on the design of reducing the group velocity mismatch between the strip waveguide and the PCW, our coupling structure requires only eight periods of PCs, a length of a few microns, to achieve efficient coupling over the entire spectrum of the guided mode.

The schematic of the slow light PCW with the PC group index taper is shown in Fig. 1(a), which comprises a standard W1 line-defect-induced PCW with a unified lattice constant of $a=405$ nm. The silicon slab thickness and the air hole diameters are chosen to be $h=230$ nm and $d=180$ nm, respectively, such that the W1 PCW supports single mode operation. The dispersion relation (photonic band diagram) of the defect-guided mode is calculated using a three-
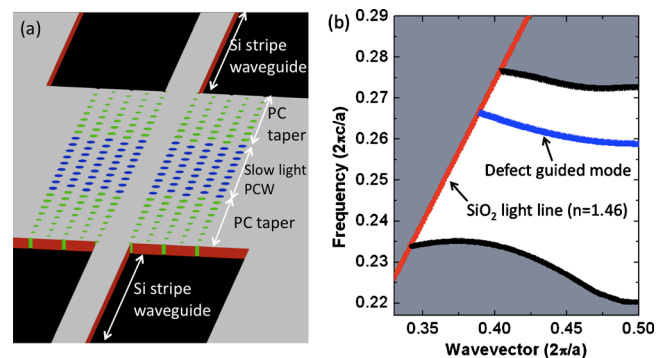

FIG. 1. (Color online) (a) Schematic of the device structure which shows input and output strip waveguides, PC taper with gradually changing hole sizes (not to scale), and the central region that supports the slow light mode. (b) Dispersion relation of the defect-guided mode in the slow light PCW, as highlighted in (a).

a)Electronic mail: cheyunlin@mail.utexas.edu.
b)Electronic mail: alan.wang@omegaoptics.com.
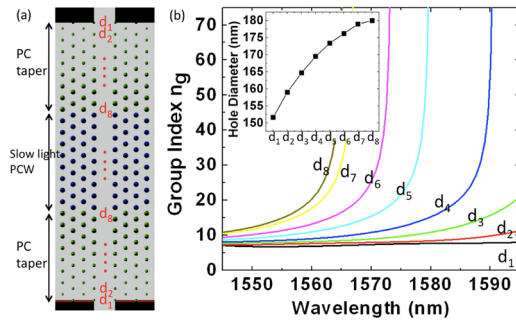c)Electronic mail: raychen@uts.cc.utexas.edu.

FIG. 2. (Color online) (a) Schematic showing different hole diameters of the PC taper and the slow light PCW. (b) Group index (n_g) vs wavelength relation for different hole diameters. The hole diameters $d_1, d_2, \ldots, d_8$ are shown in the inset.

dimensional (3D) plane-wave expansion (PWE) method as shown in Fig. 1(b). The simulated band diagram shows a guided mode from 1522 to 1567 nm, which falls inside our experiment observation window. The choice of air hole diameters (d_n, $n = 1, 2, \ldots, 8$) to create the PC tapers is based on an empirical equation $d_n = 144.15 + 8.19n - 0.46n^2$, which can create a smooth transition of hole diameters within a very short distance as shown in Fig. 2(a). To have a better understanding on the effect of PC taper, we calculate the group index (n_g) of each period of the PC taper as a function of wavelength using a 3D PWE method as shown in Fig. 2(b). One can see from the group index dispersion relation in Fig. 2(b) that this gradual increment of hole size results in a gradual increase in group index for the guided mode. Compared to butt coupling, the guided mode sees a smoother transition in group index as it enters the PCW. As a result, the guided mode coupled from the strip waveguide can slow down gradually over the eight periods of transitional region as it enters the slow light PCW. Coupling out from the slow light PCW to a strip waveguide is simply the reverse process. Under this design, the group velocity mismatch between a strip waveguide and a slow light PCW is significantly reduced, which should lead to significant improvement of coupling efficiency.

Light transmission through PCWs with and without a PC taper is verified by 2D FDTD analysis as shown in Fig. 3. Although the group index taper is only eight periods
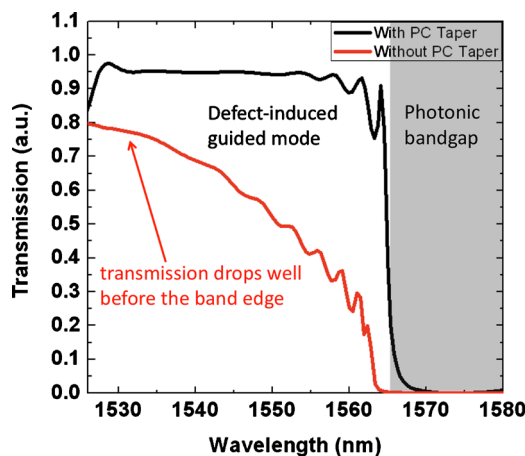

FIG. 3. (Color online) Simulated transmission spectrum using 2D FDTD analysis, comparing the coupling performance of W1 PCW with (upper curve) and without (lower curve) a PC taper.
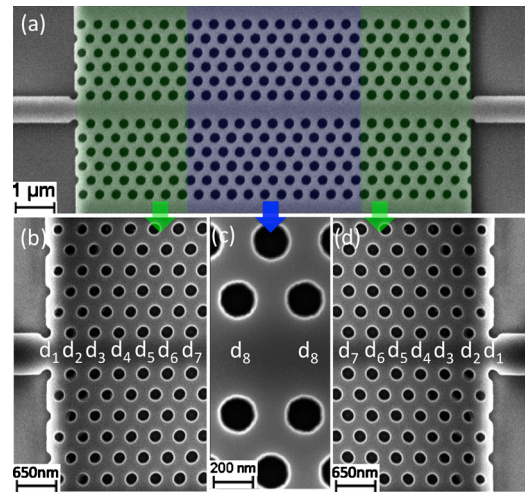

FIG. 4. (Color online) Scanning electron micrograph of the fabricated PCW structure. (a) Global look of the PCW device, which includes strip waveguide, PC taper, and a slow light PCW. [(b) and (d)] Enlarged view of the eight periods of PC taper. (c) Enlarged view of the slow light PCW region.

(3.24 μm long) of the PCW, this coupling structure has a dramatic impact on coupling efficiency into a slow light mode. For a PCW without any PC taper, coupling efficiency starts to drop well before the band edge. By contrast, when PC taper is included in the PCW, coupling efficiency remains nearly the same as its peak value even in the slow light region. Additionally, this coupling structure reduces the fluctuation of coupling efficiency due to reduced Fabry–Perot reflections.

PCW devices were fabricated on a Unibond silicon-on-insulator wafer with a 230 nm top silicon layer and a 3 μm buried oxide (BOX) layer. 45 nm of thermal oxide was thermally grown as an etching mask for pattern transfer. PCWs, PC tapers, and strip waveguides are patterned in one step with a JEOL JBX-6000FS electron-beam lithography system followed by reactive ion etching. PCW devices were formed in a nonmembrane configuration with the patterned silicon PCW core supported by the 3 μm BOX as bottom cladding layer. The hole dimension and the width of PCWs can be precisely controlled with errors less than 2 nm and sidewall roughness ~5 nm estimated by scanning electron microscope (SEM) inspection. PCW devices with and without a PC taper were fabricated on the same chip with an identical fabrication process. SEM images of the fabricated structure are shown in Fig. 4.

To characterize the coupling performance, PCW devices were tested on a Newport six-axis auto-aligning station. Input light from a broadband amplified spontaneous emission (ASE) source (Thorlab ASE-FL7002) covering the 1520–1620 nm wavelength range was TE-polarized with a 23 dB TE/TM rejection ratio and butt-coupled to/from the device with a polarization maintaining single mode tapered lensed fiber with a mode field diameter of 3 μm. Transmitted light was analyzed with an optical spectrum analyzer (ANDO AQ6317B) with 0.04 nm resolution. The transmission spectra of PCWs with and without PC tapers were normalized to the transmission spectrum without the device as shown in Fig. 5. The transmission spectra show that the PCW devices support defect-guided modes from 1523 to 1568 nm, which agrees well with the simulated band diagram.
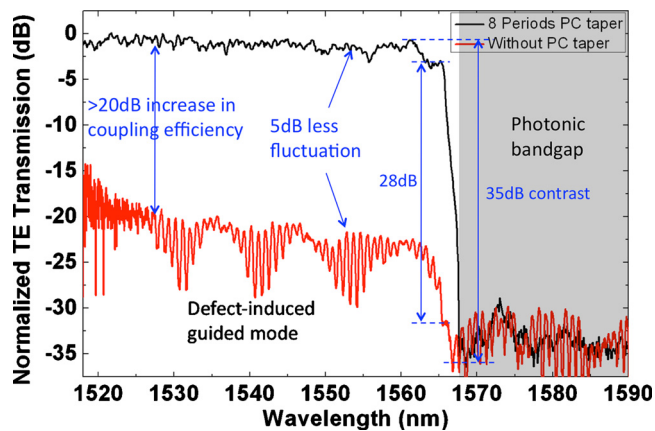
FIG. 5. (Color online) Transmission spectra comparison for W1 PCW with (upper curve) and without (lower curve) a PC taper.

Compared with direct coupling from a strip waveguide, the W1 PCW with PC taper shows several distinct improvements in the coupling efficiency. First, one can see significantly less Fabry–Perot noise when the group index tapers are added. The transmission fluctuation caused by the Fabry–Perot effect is suppressed by 5 dB throughout the defect mode. As a result, PCW with PC taper shows a nearly flat transmission. Second, the transmission is improved by more than 20 dB over the entire guided mode bandwidth of 45 nm. Third, the coupling efficiency remains very close to its peak value until 2 nm away from the photonic band gap cutoff at 1568 nm, meaning slow light modes near the band edge with very high group index can be coupled into the PCW as low group index mode. Fourth, the PC taper offers even better coupling enhancement for the band edge slow light mode. For the PCW with a PC taper, the normalized transmission at 1566 nm (2 nm from the photonic band gap) only drops 2 dB from its peak transmission, whereas it drops 10 dB without the PC taper. Under 20 dB of baseline enhancement, this translates into 28 dB improvement for the band edge slow light mode.

The limitation of this coupling approach can also be observed from the band edge cutoff behavior. One may notice that the slope of the transmission drop between 1566 and 1568 nm has two distinct regions. The first region from 1566 to 1567.5 nm shows a 25 dB drop in transmission within 1.5 nm, indicating this coupling mechanism starts to reach its limitation when group velocity slows rapidly as a function of wavelength. The second region from 1566.5 to 1567 nm shows a 10 dB drop in transmission in just 0.5 nm, which is likely due to the very high propagation loss associated with extremely high group index.

In conclusion, we present the design and experimental results of efficient coupling into a PCW using PC tapers based on matching the group velocity between a conventional strip waveguide and a slow-light PCW. Experiments show good coupling efficiency can be maintained to the PC band edge regardless of the group velocity of the guided mode by using only eight periods of PC taper. Compared to a PCW without a PC taper, measurements show a 20 dB baseline improvement in coupling efficiency, 5 dB less fluctuation, and a 28 dB enhancement for the slow light mode using only 3.24 μm long of PC taper. The experimental result also shows that less than 10 μm of PCW is needed to create a 35 dB contrast in transmission. Such a PCW structure could serve as the stepping-stone toward building ultra-compact photonic devices for on-chip optical interconnects.

[1] T. Baba, Nat. Photonics **2**, 465 (2008).
[2] M. Povinelli, S. Johnson, and J. Joannopoulos, Opt. Express **13**, 7145 (2005).
[3] D. M. Beggs, T. P. White, L. O'Faolain, and T. F. Krauss, Opt. Lett. **33**, 147 (2008).
[4] Y. Jiang, W. Jiang, L. Gu, X. Chen, and R. T. Chen, Appl. Phys. Lett. **87**, 221105 (2005).
[5] L. Gu, W. Jiang, X. Chen, L. Wang, and R. T. Chen, Appl. Phys. Lett. **90**, 071105 (2007).
[6] J.-M. Brosi, C. Koos, L. C. Andreani, M. Waldow, J. Leuthold, and W. Freude, Opt. Express **16**, 4177 (2008).
[7] X. Wang, S. Chakravarty, B. S. Lee, C.-Y. Lin, and R. T. Chen, Opt. Lett. **34**, 3202 (2009).
[8] C.-Y. Lin, X. Wang, S. Chakravarty, B. S. Lee, W. Lai, J. Luo, A. K.-Y. Jen, and R. T. Chen, Appl. Phys. Lett. **97**, 093304 (2010).
[9] Y. A. Vlasov and S. J. McNab, Opt. Lett. **31**, 50 (2006).
[10] Y. A. Vlasov, M. O'Boyle, H. F. Hamann, and S. J. McNab, Nature (London) **438**, 65 (2005).
[11] C. M. de Sterke, J. Walker, K. B. Dossou, and L. C. Botten, Opt. Express **15**, 10984 (2007).
[12] N. Ozaki, Y. Kitagawa, Y. Takata, N. Ikeda, Y. Watanabe, A. Mizutani, Y. Sugimoto, and K. Asakawa, Opt. Express **15**, 7974 (2007).
[13] J. P. Hugonin, P. Lalanne, T. P. White, and T. F. Krauss, Opt. Lett. **32**, 2638 (2007).
[14] S. G. Johnson, P. Bienstman, M. A. Skorobogatiy, M. Ibanescu, E. Lidorikis, and J. D. Joannopoulos, Phys. Rev. E **66**, 066608 (2002).
[15] S. Assefa, P. T. Rakich, P. Bienstman, S. G. Johnson, G. S. Petrich, J. D. Joannopoulos, L. A. Kolodziejski, E. P. Ippen, and H. I. Smith, Appl. Phys. Lett. **85**, 6110 (2004).
[16] Ph. Lalanne and A. Talneau, Opt. Express **10**, 354 (2002).
[17] P. Pottier, M. Gnan, and R. M. De La Rue, Opt. Express **15**, 6569 (2007).